Biomaterials 33 (2012) 418–427

Contents lists available at SciVerse ScienceDirect

Biomaterials

journal homepage: www.elsevier.com/locate/biomaterials

A graphene-based platform for induced pluripotent stem cells culture and differentiation

G.-Y. Chen [a,1], D.W.-P. Pang [a,1], S.-M. Hwang [b], H.-Y. Tuan [a,*], Y.-C. Hu [a,*]

[a] Department of Chemical Engineering, National Tsing Hua University, Hsinchu 300, Taiwan
[b] Bioresource Collection and Research Center, Food Industry Research and Development Institute, Hsinchu 300, Taiwan

ARTICLE INFO

Article history:
Received 9 September 2011
Accepted 27 September 2011
Available online 19 October 2011

Keywords:
Graphene
Graphene oxide
Induced pluripotent stem cells
Differentiation
Proliferation
Stem cells

ABSTRACT

Induced pluripotent stem cells (iPSCs) hold great promise as a cell source for regenerative medicine yet its culture, maintenance of pluripotency and induction of differentiation remain challenging. Conversely, graphene (G) and graphene oxide (GO) have captured tremendous interests in the fields of materials science, physics, chemistry and nanotechnology. Here we report on that G and GO can support the mouse iPSCs culture and allow for spontaneous differentiation. Intriguingly, G and GO surfaces led to distinct cell proliferation and differentiation characteristics. In comparison with the glass surface, iPSCs cultured on the G surface exhibited similar degrees of cell adhesion and proliferation while iPSCs on the GO surface adhered and proliferated at a faster rate. Moreover, G favorably maintained the iPSCs in the undifferentiated state while GO expedited the differentiation. The iPSCs cultured on both G and GO surfaces spontaneously differentiated into ectodermal and mesodermal lineages without significant disparity, but G suppressed the iPSCs differentiation towards the endodermal lineage whereas GO augmented the endodermal differentiation. These data collectively demonstrated that the different surface properties of G and GO governed the iPSCs behavior and implicate the potentials of graphene-based materials as a platform for iPSCs culture and diverse applications.

1. Introduction

Graphene is an atomic-thick sheet of carbon atoms arranged in two-dimensional (2D) honeycomb structure with unique physical, chemical and mechanical properties [1,2]. The capability of bio-functionalization of graphene and its derivative, graphene oxide (GO), has brought these nanomaterials under spotlight and has drawn intense attention for a plethora of applications in biotechnology including bioassays [3], biosensors [4], photothermal anti-cancer therapy [5] and electrical stimulation of cells [6]. Thanks to the biocompatibility at low concentration [7] and 2D nature with ultra-large surface area, graphene and GO have recently captured interests as cell culture substrates. Substrates coated with graphene or GO have enabled the culture of several mammalian cells including NIH-3T3 fibroblast [8] and A549 [9], but the widespread use of graphene and GO for cell culture necessitates more intensive research.

Induced pluripotent stem cells (iPSCs) are pluripotent cells that can be derived from somatic cells by introducing a cocktail of reprogramming factors while obviating the need to destroy embryos [10,11]. Similar to embryonic stem (ES) cells, iPSCs can be maintained in the undifferentiated state indefinitely but can differentiate into cells belonging to all 3 germ layers: endoderm (e.g. hepatocytes, insulin-producing β cells and lung epithelium), mesoderm (e.g. osteoblast and chondrocytes) and ectoderm (e.g. neural cells). The pluripotency and avoidance of ethical issues render iPSCs a promising cell source for the regeneration of virtually all tissues/organs and their potentials in disease modeling [12] as well as the treatment of various diseases including Parkinson's diseases [13], hemophilia [14] and sickle cell anemia [15] have been implicated. To maintain the pluripotency, iPSCs typically need to be cultured on the feeder layer cells (e.g. mouse embryonic fibroblasts) with appropriate cytokines such as leukemia inhibitory factor (LIF) [16]. Without these supporting cell/matrix and anti-differentiation factors, iPSCs in 2D or in suspension cultures spontaneously differentiate *in vitro* and form 3D aggregates known as embryoid bodies (EBs) which encompass cells of endodermal, mesodermal and ectodermal lineages. As differentiation continues, a variety of cell types are developed within the EBs environment.

Given the promise of iPSCs in regenerative medicine and graphene-based materials as biomaterials, the overriding objectives of this study were to evaluate the feasibility of culturing iPSCs

* Corresponding authors. Tel.: +886 3 571 8245/572 3661; fax: +886 3 571 5408.
E-mail addresses: yuchen@che.nthu.edu.tw, hytuan@che.nthu.edu.tw (Y.-C. Hu).
[1] These two authors contributed equally to this work.

0142-9612/$ – see front matter © 2011 Elsevier Ltd. All rights reserved.
doi:10.1016/j.biomaterials.2011.09.071

on the surface of G- and GO-coated substrates, and to assess how the surface properties dictated the iPSCs proliferation and differentiation.

2. Materials and methods

2.1. Preparation of graphene oxide (GO)

All of the chemicals were used as received. GO was prepared by oxidation and exfoliation of commercially available graphite by Hummer's method. Briefly, 0.5 g of natural graphite (Bay Carbon, SP-1) and 0.5 g of sodium nitrate ($NaNO_3$, J. T. Baker) was mixed in a 500 ml round bottom flask, followed by the addition of concentrated sulfuric acid (95–97%, Sigma–Aldrich) and stirring on ice. When the temperature dropped to 0 °C, 3 g of potassium permanganate ($KMnO_4$, J. T. Baker) was slowly added to the solution and the mixture was moved to the warm water bath at 40 °C. After stirring for 1 h, the solution was added with 30 ml of deionized water, stirred for another 30 min, further diluted by 100 ml of deionized water and followed by subsequent drop by drop addition of 3 ml of hydrogen peroxide (30% in water, Sigma–Aldrich). The solution was filtered and washed until the filtrate became pH neutral. Finally, the filter cake was sonicated in deionized water for 30 min to obtain the single layer GO dispersion (1.5 mg/ml).

2.2. Preparation of GO- and graphene (G)-coated substrates for iPSCs culture

Coating of glass coverslips with GO was performed as described below. For substrate cleaning, the 22 mm × 22 mm glass coverslip was first immersed into the piranha solution (hydrogen peroxide/sulfuric acid at a volumetric ratio of 1:3) for 10 min at 120 °C, washed with ethanol and water sequentially and then blown dried by nitrogen gas. The cleaned coverslip was then immersed in 3% toluene solution of 3-aminopropyltriethoxysilane (3-APTES) for 30 min, washed with toluene, ethanol and water sequentially, followed by blow-drying and baking with nitrogen at 125 °C for functionalization. GO was immobilized on a coverslip surface by immersing the functionalized glass coverslip into the GO solution (1.5 mg/ml) for 1 h.

G-coated coverslips were obtained by immersing the GO-coated coverslips into the 20% N,N-dimethylformamide (DMF, Sigma–Aldrich) solution of hydrazine monohydrate (Alfa Aesar) at 80 °C for 24 h, after which the color of the coverslips transformed from yellowish brown to greyish black due to the reduction of GO to G.

2.3. Characterization

The attenuated total reflectance Fourier transform infrared (ATR-FTIR) spectra of G and GO were recorded on a Perkin Elmer RXI equipped with an ATR stage. The ATR-FTIR spectra were acquired from 1000 to 3750 cm^{-1} with 1 cm^{-1} resolution by 64 scans. UV–Vis transmittance spectra of the coated substrates were analyzed using a Hitachi U-4100 spectrophotometer. The surface morphology of G- and GO-coated substrates was revealed using a Hitachi S-4800 field emission scanning electron microscope (FE-SEM). Topology profiles of G and GO were examined on an atomic force microscope (AFM, XE-70, Park System) using the aluminum coating silicon probe (resonant frequency = 300 kHz, force constant = 40 N/m) working under tapping mode (scanning rate = 1 Hz). High-resolution X-ray photoelectron spectroscopy (HR-XPS) measurements were performed using a PHI Quantera SXM.

2.4. Mouse iPSCs culture

Mouse iPSCs cell line 20D17 was kindly supplied by Dr. Shinya Yamanaka (Center for iPS Cell Research and Application, Kyoto University) and harbored the gene encoding green fluorescent protein (GFP) under the control of Nanog promoter as the pluripotency marker [10]. The mouse embryonic fibroblasts (MEF, Food Industry Research and Development Institute, Taiwan) were cultured and treated with mitomycin C as the feeder cells following standard protocols [17]. For iPSCs expansion, iPSCs were thawed, seeded onto the MEF cells in T75 flasks and cultured using high glucose DMEM (without sodium pyruvate, Gibco) supplemented with 15% fetal bovine serum (FBS, Gibco), 0.1 mM non-essential amino acid (Gibco), 0.1 mM 2-mercaptoethanol (Gibco) and 1000 U/ml mouse leukemia inhibitory factory (LIF, Millipore). The cells continued to be cultured with daily medium exchange and subcultured at ≈70–80% confluency by trypsinization.

2.5. Cells adhesion, proliferation and colony formation

To seed the iPSCs on the uncoated, G-coated and GO-coated glass coverslips, the iPSCs and feeder cells were trypsinized, seeded to T75 flasks coated with 0.1% gelatin and incubated at 37 °C for 40 min [18]. After the MEF cells attached, the iPSCs in suspension were removed and resuspended in the medium as mentioned above. The cells were then seeded onto the substrates (1×10^4 cells/cm^2) in the 6-well plates and cultured in the medium (2 ml/well) supplemented with LIF (1000 U/ml) to maintain the cells in the undifferentiated state. The cells were trypsinized the next day (day 1) or at day 3 and counted with the hemacytometer. In parallel, the cell morphology and colony formation were observed under the phase contrast microscope at days 1, 3 and 5.

2.6. Immunohistochemical staining and confocal microscopy

To monitor the cellular differentiation, the cells were cultured on the 3 different substrates using the medium without LIF to allow for simultaneous differentiation, and GFP expression by the iPSCs was monitored by the confocal microscope at days 5 and 9 after counterstaining with 4,6-diamidino-2-phenylindole (DAPI, Vector Labs). Alternatively, the cells were washed with phosphate buffered-saline (PBS), fixed with 4% formaldehyde, treated with 0.5% Tween 20 and subjected to immunohistochemical staining specific for Nanog or Oct4 following standard procedures. The primary antibodies were rabbit anti-mouse monoclonal antibodies specific for Nanog (1:100 dilution, ab80892, Abcam) and Oct4 (1:100 dilution, ab19857, Abcam) while the secondary antibody was goat anti-rabbit antibody conjugated with Alexa fluor 532 (1:100 dilution, A11009, Invitrogen). After counterstaining with DAPI, the cells were observed under the confocal microscope.

2.7. Quantitative real-time reverse transcription polymerase chain reaction (qRT-PCR)

To quantify the gene expression levels, the iPSCs cultured on the 3 different substrates were trypsinized at days 5 and 9. Total RNA was extracted using RNeasy Mini Kit (Qiagen) and reverse transcribed to complementary DNA (cDNA) using the Reverse Transcriptase 1st-Strand cDNA Synthesis Kit (Epicentre Biotechnologies). The primer sequences specific for the pluripotency markers (*Nanog* and *Oct4*), endodermal markers (*Gata4* and *Ihh*), ectodermal markers (*Fgf5* and *Nestin*), mesodermal markers (*T* and *BMP4*) and the internal control gene *gapdh* used for qRT-PCR are listed in Supplementary Table S1. The cDNA was subject to quantitative real-time PCR (Q-PCR) in an ABI 7300 real-time PCR system (Applied Biosystems) with SYBR Green PCR master mix (Applied Biosystems) using the primers targeting the respective genes, under the following conditions: 2 min at 50 °C, 10 min at 95 °C, and then 40 cycles of 15 s at 95 °C and 1 min at 60 °C. For each real-time PCR, a no-template reaction was included as the negative control. The threshold cycle values for the target gene and *gapdh* were obtained from Q-PCR reactions and converted to the gene copy numbers from the standard curves. The copy number ratios of the target gene to *gapdh* were calculated.

2.8. Gene transfer analysis

The iPSCs on the 3 different substrates were transduced with a baculovirus expressing DsRed (a red fluorescent protein) under the control of CAG promoter when the cell density reached ≈2×10^4 cells/cm^2. Based on the multiplicity of infection (MOI), a certain volume of virus supernatant was pre-mixed with $NaHCO_3$-deficient DMEM containing 10% FBS to adjust the final volume to 500 μl (per well) [19]. The cells on the substrates (in the 6-well plates) were washed with PBS and the transduction was initiated by adding the virus mixture to the cells, followed by gentle shaking on the rocking plate for 4 h at room temperature. After the incubation period, the cells were washed with PBS and continued to be cultured. One day later, the cells were subjected to confocal microscopy to examine the DsRed expression. Alternatively, the cells were trypsinized to measure the percentage of DsRed-expressing cells and mean fluorescence intensity (FI) by flow cytometry as described previously [20]. Total FI was yielded by multiplying the percentage of DsRed-positive cells by the mean FI.

2.9. Statistical analysis

All data were analyzed using Student's *t*-tests and are expressed as mean values of 3 independent experiments. *p* values less than 0.05 were considered significant.

3. Results

3.1. Preparation and characterization of G- and GO-coated substrates

GO sheets were prepared by Hummer's method and the presence of epoxide, hydroxyl, carbonyl and carboxyl groups was confirmed by FTIR and XPS (Fig. 1a–c). AFM images revealed that they were mostly single-layered with lateral size ranging from 2 to 6 μm (Fig. 2a,b). For iPSCs culture, GO was tightly immobilized onto clean glass coverslips. G-coated coverslips were obtained via direct hydrazine reduction of GO sheets. SEM (Fig. 3) and AFM (Fig. 4) images of G and GO sheets immobilized on the silicon substrate revealed uniform and dense coverage of thin sheets on the surface. The surface roughness (the root-mean-square deviation (R_q)), was 0.969 nm and 1.031 nm for G

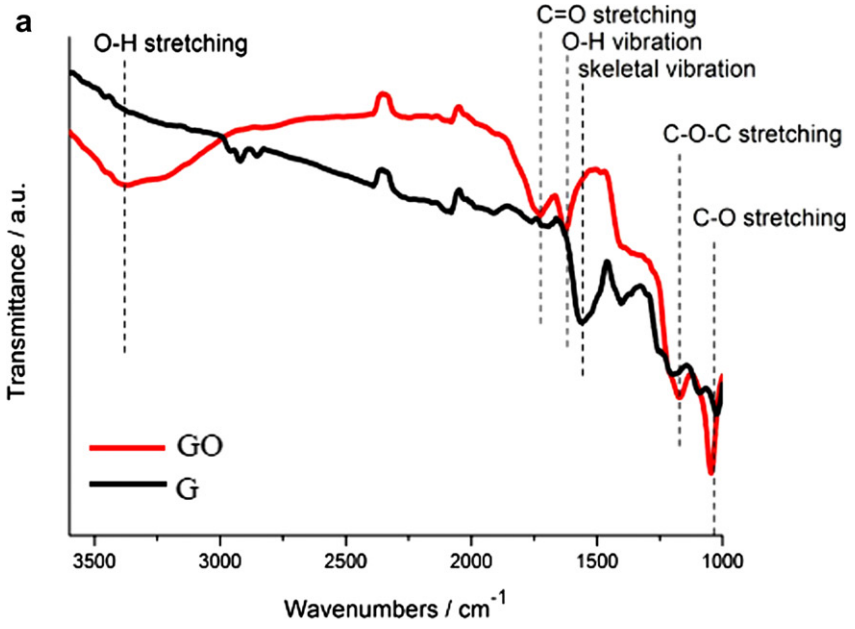
a
O-H stretching
C=O stretching
O-H vibration
skeletal vibration
C-O-C stretching
C-O stretching
Transmittance / a.u.
GO
G
3500
3000
2500
2000
1500
1000
Wavenumbers / cm-1

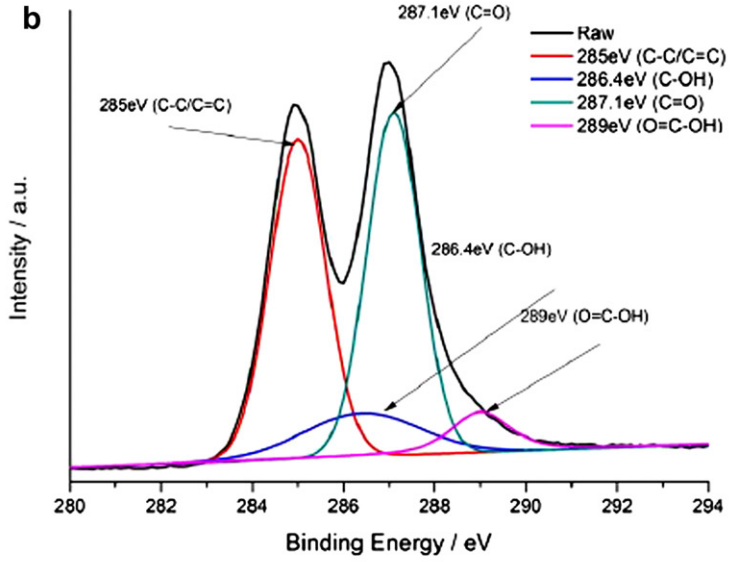
b
287.1eV (C=O)
Raw
285eV (C-C/C=C)
286.4eV (C-OH)
287.1eV (C=O)
289eV (O=C-OH)
285eV (C-C/C=C)
286.4eV (C-OH)
289eV (O=C-OH)
Intensity / a.u.
280
282
284
286
288
290
292
294
Binding Energy / eV

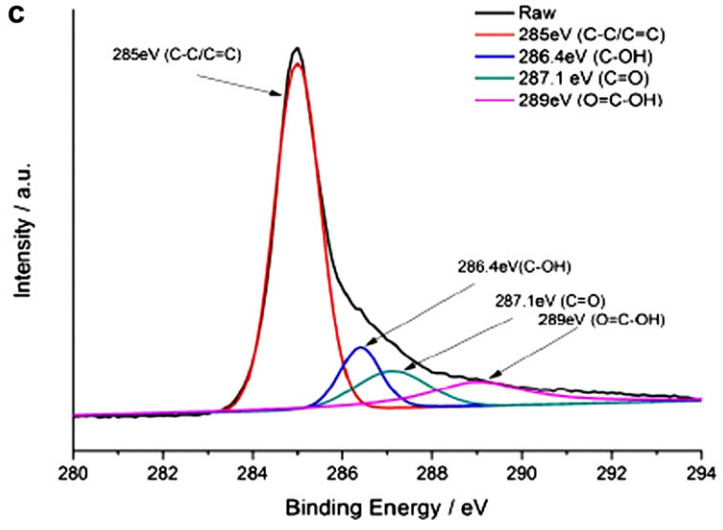
c
Raw
285eV (C-C/C=C)
286.4eV (C-OH)
287.1 eV (C=O)
289eV (O=C-OH)
285eV (C-C/C=C)
286.4eV(C-OH)
287.1eV (C=O)
289eV (O=C-OH)
Intensity / a.u.
280
282
284
286
288
290
292
294
Binding Energy / eV

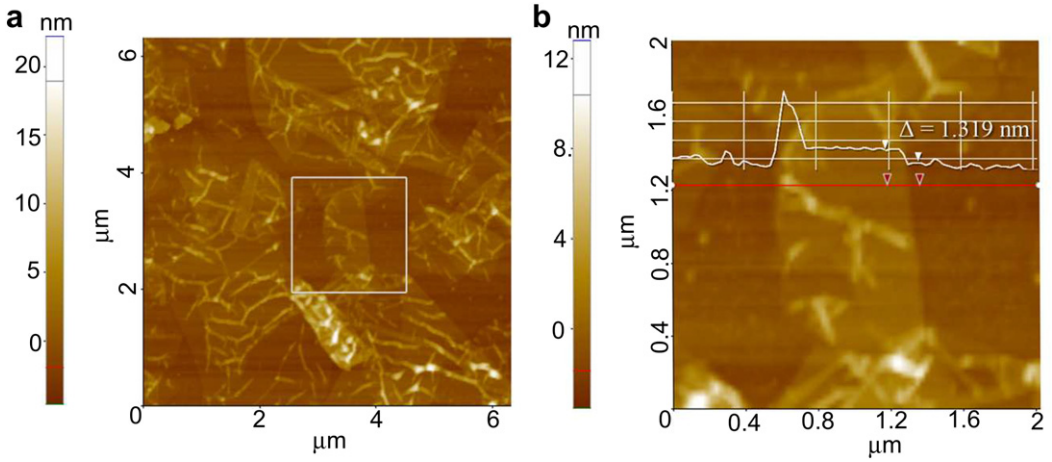

Fig. 2. AFM analyses of GO. (a) Images of as-prepared GO on a silicon substrate. (b) Height profile of the square area shown in (a). The lateral size of GO was ≈2–6 μm. Height difference between the GO sheet and substrate (the cursor pair in (b)) was 1.319 nm, consistent with the thickness of the single layer GO sheet. The crumpled silk wave observed under the AFM was characteristic of very thin sheets of GO layer covered on the substrate.

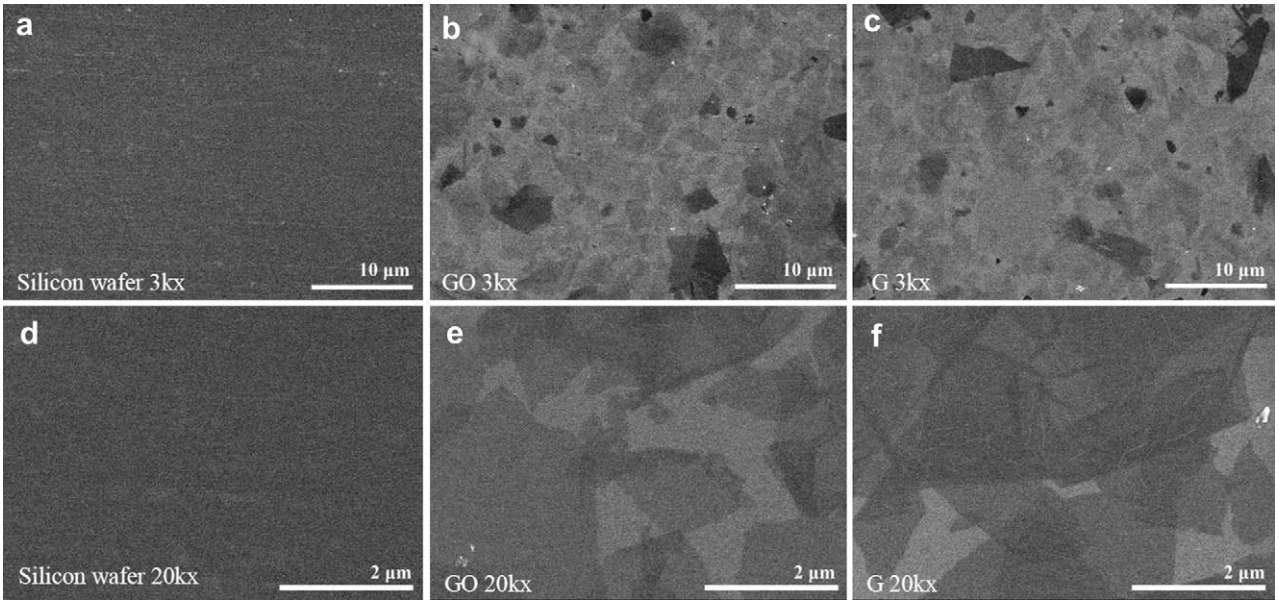

Fig. 3. SEM images of GO and G. (a, d) Silicon wafer, (b, e) GO and (c, f) G on the silicon substrate. Dense coverage of GO and G on the substrate is revealed in (b, c). The thin sheet morphology of GO and G is clearly observed in (e, f).

and GO-coated substrates, respectively, without significant difference (Supplementary Table S2). Both G- and GO-coated glass coverslips exhibited high transparency feature (Fig. 5a) with transmittance exceeding 90% between 400 and 800 nm (Supplementary Figure S1).

3.2. iPSCs culture on the G- and GO-coated substrates

To evaluate whether G- and GO-coated glass substrates enabled the iPSCs culture, the mouse iPSCs (kindly provided by Prof. Shinya Yamanaka, Kyoto University) were seeded at the same density (1×10^4 cells/cm^2) and cultured in the LIF-containing medium. Quantitative analyses of cell densities on the coverslips (Fig. 5b) depicted that iPSCs adhered to the 3 different substrates 1 day after seeding. However, the cell densities on the glass and G-coated glass ($\approx 4 \times 10^3$ cells/cm^2) were lower than that on the GO surface ($\approx 7.9 \times 10^3$ cells/cm^2), suggesting less efficient cell adherence onto the glass and G surfaces. The cells grew ≈9–10-fold to ≈ 3.5–4.0×10^4 cells/cm^2 at day 3 on the glass and G surfaces, but proliferated more rapidly on the GO surface to $\approx 8.4 \times 10^4$ cells/cm^2 (≈11-fold proliferation).

Fig. 1. FTIR spectra (1000–3750 cm^{-1}) and XPS spectra of GO and G. (a) FTIR spectra. (b) XPS spectra of GO, (c) XPS spectra of G. The FTIR absorption bands at 1042 cm^{-1} and 1730 cm^{-1} demonstrated C–O and C=O stretching of COOH group, respectively; the 1620 cm^{-1} band indicated the absorptions of O–H bending vibration, epoxide groups and skeletal ring vibrations; C–O vibration band of epoxide groups was shown at 1170 cm^{-1}. In the G spectrum, a new band of 1560 cm^{-1} was attributed to the skeletal vibration of G sheets, indicating the higher degree of graphitic domain. The GO spectrum showed a more prominent broad peak than G spectrum near 3380 cm^{-1} due to the O-H stretching vibration and the resultant adsorbed water molecules on the GO surface. The deconvolution spectrum of GO showed four different peaks centered at 285 eV, 286.4 eV, 287.1 eV and 289 eV, which corresponded to C–C/C=C, C–OH, C=O and O=C–OH, respectively. Except the aromatic C–C/C=C at 285 eV, peaks were diminished in the case of G, confirming the reduction of GO to G.

One advantage of our methodology for preparing the G- and GO-coated substrates is the resultant high transparency that allowed for direct microscopic observation (Fig. 5c), which attested the cell adherence to the 3 surfaces at day 1 and formation of colonies with distinct sizes and appearances at day 3. The colonies on the glass resembled the undifferentiated cells as judged from the tightly packed cells and distinct colony border. In contrast, the cell aggregates were irregular in shape on the G surface and exhibited pronounced outgrowth on the GO surface (Fig. 5c). At day 5, EBs formation was observed on all 3 substrates. However, the EBs on the GO surface were strikingly larger in size, which was concomitant with the higher initial cell density attached to the GO surface, a phenomenon also observed for EBs formed on the collagen/Matrigel surface [21]. These data collectively demonstrated that G and GO were biocompatible with iPSCs and supported iPSCs attachment and proliferation.

3.3. iPSCs differentiation on the G- and GO-coated substrates

How G and GO influenced the iPSCs differentiation was assessed by culturing the cells on the 3 substrates without LIF. Since the iPSCs were engineered to express green fluorescent protein (GFP) under the control of Nanog promoter as a pluripotency marker [10], the spontaneous cellular differentiation was first examined by confocal microscopy (Fig. 6a). At day 5 the majority of cells (as counterstained by 4,6-diamidino-2-phenylindole (DAPI)) on all 3 substrates remained GFP-positive, but at day 9 considerable amounts of cells on the glass lost the GFP expression. Conversely, at day 9 GFP expression remained evident on G but extinguished in most cells on GO, suggesting that the cells on the glass and GO spontaneously lost the pluripotency, while G appeared to impede the differentiation.

To quantify the loss of pluripotency, the mRNA levels of two pluripotency markers (Nanog and Oct4) were measured by quantitative real-time reverse transcription polymerase chain reaction

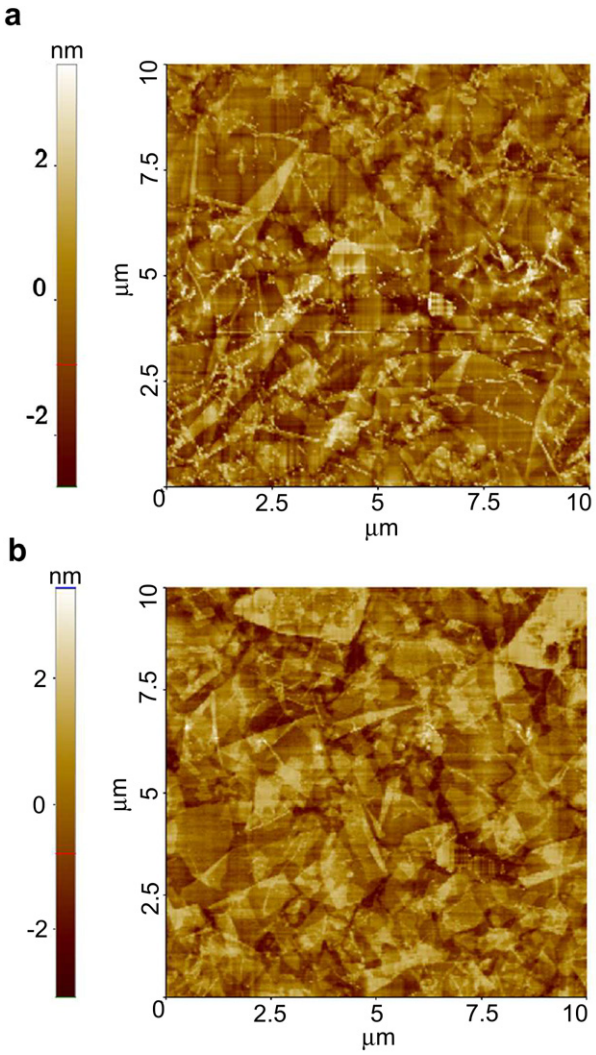

Fig. 4. AFM images of (a) GO and (b) G sheets immobilized on silicon substrates. Surface roughness parameters, including the average deviation from mean (R_a), the root–mean-square deviation (Rq) and the peak-to-peak distance (R_z), are shown in Table S2.

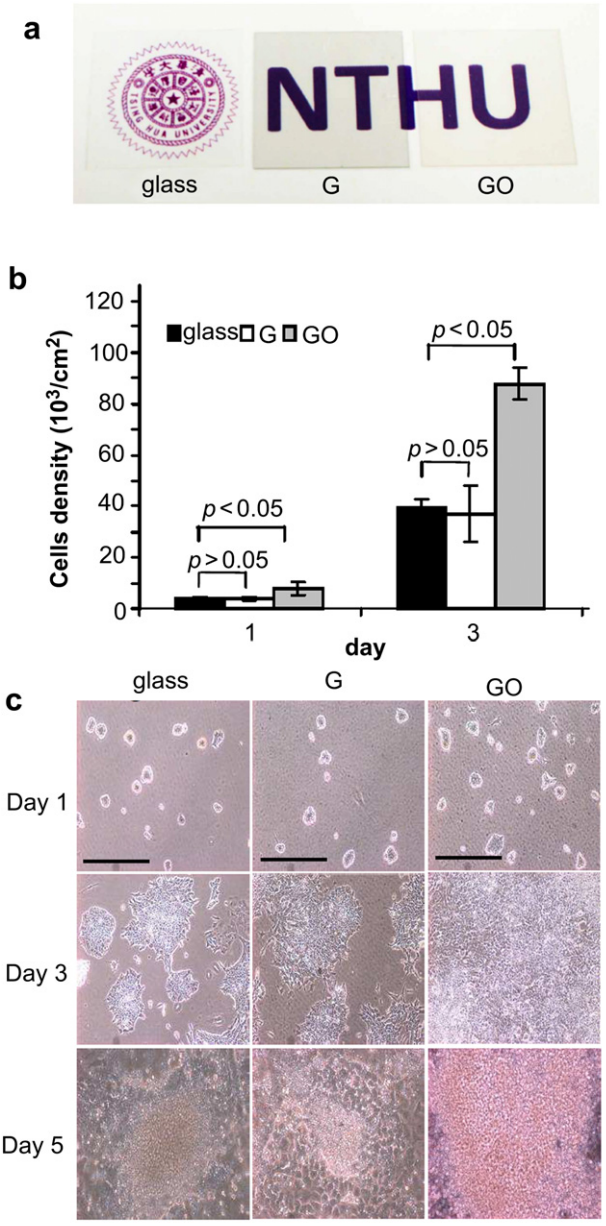

Fig. 5. G and GO enabled iPSCs attachment and proliferation. (a) Photograph of blank, G- and GO-coated glass coverslips, (b) cell growth, (c) cell morphology. The cells were seeded at the same density (1×10^4 cells/cm^2) onto the unmodified, G-coated and GO-coated coverslips and cultured in the LIF-containing medium to facilitate the maintenance of undifferentiated state. Bar, 100 μm.

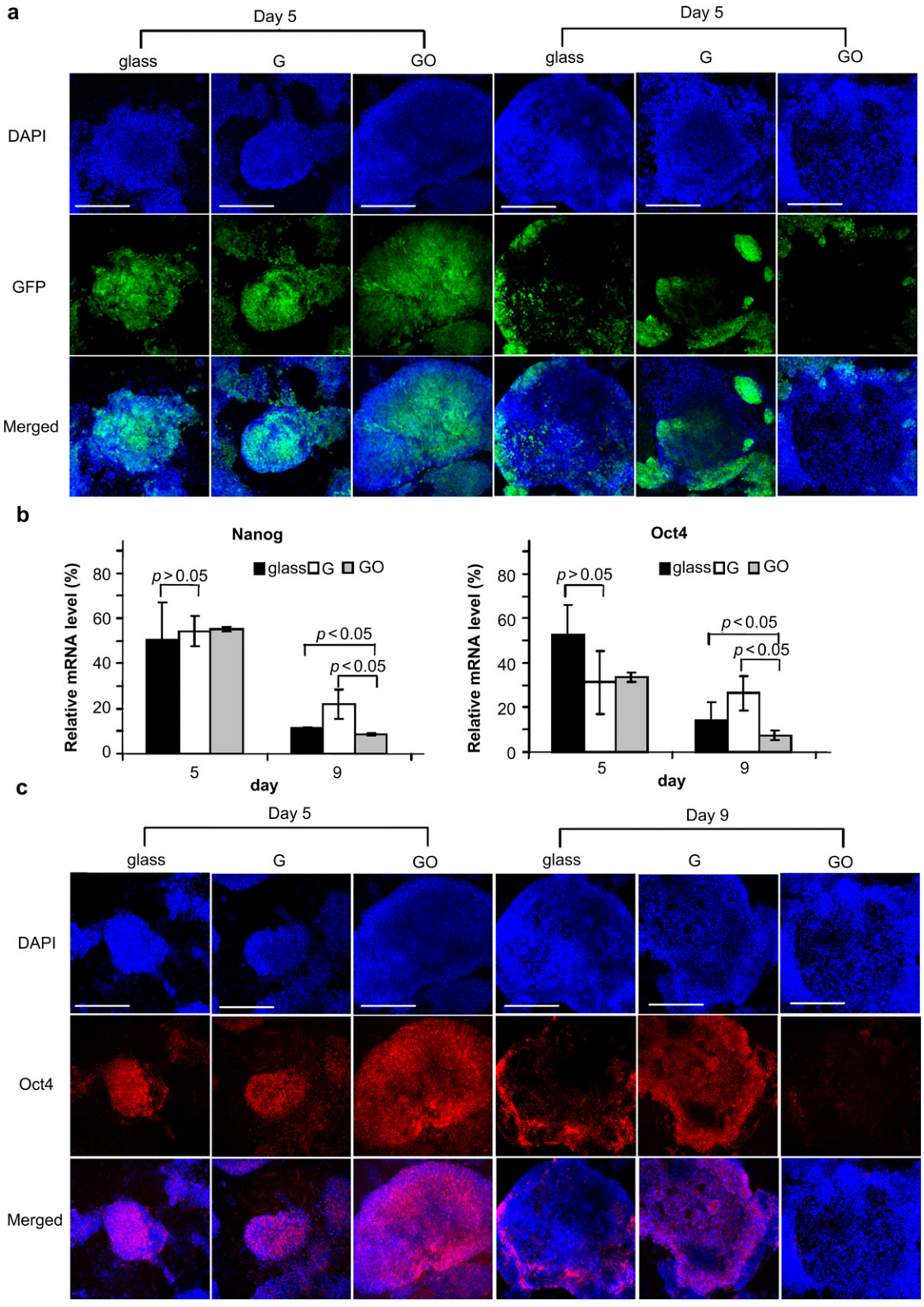

Fig. 6. G and GO led to differences in the iPSCs differentiation state. (a) Confocal microscopic observation of GFP expression. (b) mRNA levels of pluripotency markers Nanog and Oct4. (c) Immunohistochemical staining against Oct4. iPSCs were cultured on the 3 different substrates and analyzed at days 5 and 9. For confocal microscopy, the cells were counterstained by DAPI. Bar, 100 μm.

(qRT-PCR). Compared with the expression at day 1 (defined as 100%), the Nanog expression for the 3 groups declined to ≈50%–55% at day 5 without statistical difference (Fig. 6b). However, at day 9 the Nanog expression on G (≈22%) was significantly ($p < 0.05$) higher than those on the glass (≈11%) and GO (≈8%). A similar trend in the Oct4 expression was also observed (Fig. 6b).

To verify the findings in the protein level, immunohistochemical staining specific for Nanog and Oct4 was performed. Fig. 6c illustrates evident Oct4 expression on all 3 substrates at day 5 and markedly decayed expression on the glass at day 9. The Oct4 expression remained strikingly high on G but was barely detectable on GO. Similar staining patterns of Nanog-expressing cells were also noted on the 3 surfaces (Supplementary Figure S2). Together with the GFP expression and qRT-PCR data, these data unveiled that G and GO gave rise to disparity in the pluripotent states of iPSCs.

To assess whether iPSCs on the G and GO substrates equally differentiated towards the 3 germ layers, the mRNA levels of the lineage-specific genes were measured by qRT-PCR at days 5 and 9,

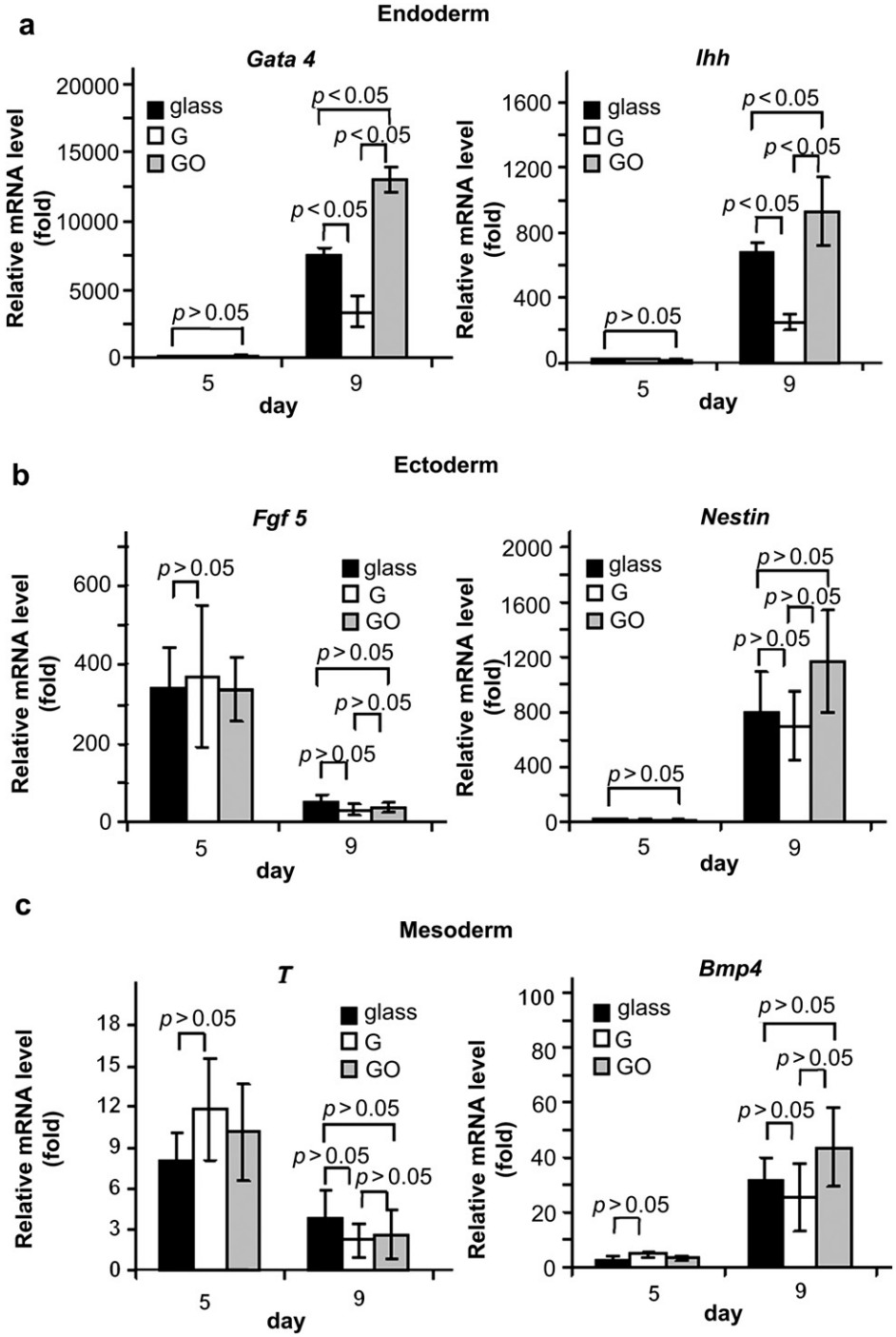

Fig. 7. G and GO resulted in discrepancies in the iPSCs propensity of differentiation. iPSCs were cultured on the 3 different substrates and analyzed for the expression levels of lineage-specific marker genes: (a) endodermal markers (*Gata4* and *Ihh*), (b) ectodermal markers (*Fgf5* and *Nestin*) and (c) mesodermal markers (*T* and *Bmp4*). The expression levels were measured by qRT-PCR and normalized against those at day 1.

which were normalized against those at day 1. As delineated in Fig. 7a, the expression levels of endodermal markers *Gata4* and *Ihh* on all 3 substrates remained similarly low at day 5, but increased sharply at day 9. In comparison with the glass, at day 9 G significantly ($p < 0.05$) reduced the *Gata4* and *Ihh* expression levels whereas GO enhanced the *Gata4* and *Ihh* expression, indicating that the differentiation along the endodermal pathway was mitigated on G but was promoted on GO.

When the ES cells differentiate along the ectodermal pathway, *Fgf5* expression ascends early in the differentiation (e.g. at day 5) and then descends, but *Nestin* expression rises and decreases at a later time point [22]. Concurrent with this temporal expression pattern, on all 3 substrates *Fgf5* expression was upregulated at day 5 and then plummeted at day 9, yet *Nestin* expression was not elevated until day 9 (Fig. 7b). The differences in the expression levels between the 3 substrates were statistically insignificant ($p > 0.05$), indicating similar degrees of ectodermal differentiation. Upon ES cells differentiation along the mesodermal pathway, the expression of lineage-specific marker *T* culminates at day 5 [23], while the *Bmp4* expression commences at day 5 and continues to ascend as the differentiation progresses [24]. Fig. 7c depicts that the mesodermal marker genes *T* and *Bmp4* exhibited the aforementioned temporal expression profiles without significant differences ($p > 0.05$) among the 3 substrates, underscoring that the iPSCs cultured on the 3 substrates differentiated towards the mesodermal pathway in a similar fashion.

3.4. Gene transfer into iPSCs on the G- and GO-coated substrates

iPSCs hold great promise for regenerative medicine as the cellular differentiation can be guided by exogenous factors/cues or by genetic modification [25]. To examine whether the iPSCs on the 3 substrates were amenable to gene transfer, the cells were transduced with a recombinant baculovirus (an effective viral vector for gene delivery into mammalian cells [26,27]) expressing the red fluorescent protein. Fig. 8 reveals that the iPSCs cultured on the 3 substrates were transduced by baculovirus with similar efficiencies, indicating that G and GO substrates neither undermined nor enhanced the iPSCs capability for exogenous gene uptake. This finding contradicted with the previous report that the transfection efficiency of NIH-3T3 fibroblasts was elevated when the cells were cultured on the G- and GO-coated glass coverslips [8], probably due to the difference in the cell type and gene vector.

4. Discussion

In this study we unveiled that G- and GO-coated substrates are biocompatible with iPSCs and enable the cell adherence and proliferation, which supports the notions that GO exerts low cytotoxicity to mammalian cells including A549, NIH-3T3 and human fibroblasts [9,28,29] and G is biocompatible to human mesenchymal stem cells [30]. However, GO enables more favorable iPSCs adherence and proliferation than G, probably because the more abundant oxide groups on the GO surface (Fig. 1) conferred stronger hydrophilicity [31].

More strikingly, iPSCs cultured on G and GO exhibit disparities in the differentiation propensity. G hampers spontaneous differentiation (Fig. 6), especially towards the endodermal lineage (Fig. 7a). On the contrary, GO promotes the iPSCs differentiation, most pronouncedly along the endodermal pathway, although the differentiation into ectoderm and mesoderm was similar for iPSCs cultured on both G and GO (Fig. 7b and c). A variety of natural and synthetic substrates/scaffolds have been exploited for the culture of ES cells [32,33], whose lineage specification can be directed by the substrate themselves and the matrix molecules conjugated to the substrate surface. For instance, laminin promotes the ES cell differentiation towards ectodermal [34] and endodermal fates [35]. A wealth of literature also documents that such substrate properties as elasticity, stiffness, roughness, wettability, morphology [30] and topography [8] can govern the adhesion, growth and ultimate fate of stem cells. Interestingly, G-coated substrates have recently been shown to accelerate the osteogenic differentiation of human mesenchymal stem cells without harming the cell shape and attachment [30]. However, how the substrate characteristics impact on the iPSCs behavior and differentiation remains largely unknown. The only relevant study demonstrates that thicker films of multi-wall carbon nanotubes result in better iPSCs adhesion and maintenance of pluripotency than thinner films, thanks to the increased surface roughness [36]. However, the G- and GO-coated substrates are similar with regard to surface thickness, coverage and roughness (Figs. 2–4 and Supplementary Table S2) which, as such, cannot account for the disparities in iPSCs fates. Conversely, G- and GO-coated substrates differ in the abundance of polar groups (Figs. 1,2) and hydrophilicity. Given that certain functional groups (e.g. carboxylic group) can influence the ES cell differentiation [37], the difference in the surface groups might affect the types of iPSCs surface receptors that can bind to G and GO

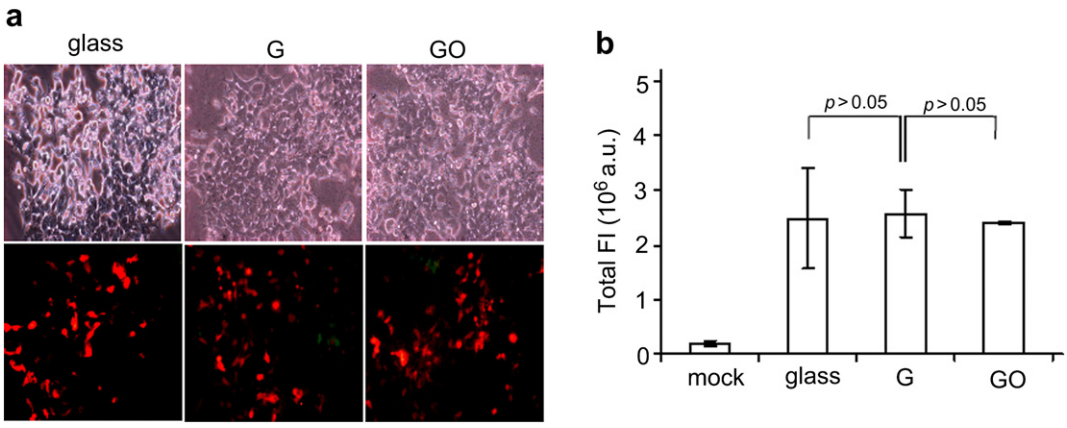

Fig. 8. iPSCs cultured on the G- or GO-coated substrates remained amenable to gene transfer. (a) Microscopic observation. (b) Quantitative analyses of gene expression. The iPSCs cultured on the 3 substrates were transduced with a recombinant baculovirus expressing DsRed and continued to be cultured. Mock-transduced cells were cultured in parallel and served as the negative control. The cells were observed under the phase contrast microscope (upper panel in (a)) or the confocal microscope (lower panel in (a)), or measured by flow cytometry for the total fluorescence intensities (FI) at 1 day post-transduction. The total FI represent the averages of 3 independent culture experiments and are expressed in arbitrary units (a.u.). The total FI are similar for the 3 groups (glass, G and GO) without statistical difference.

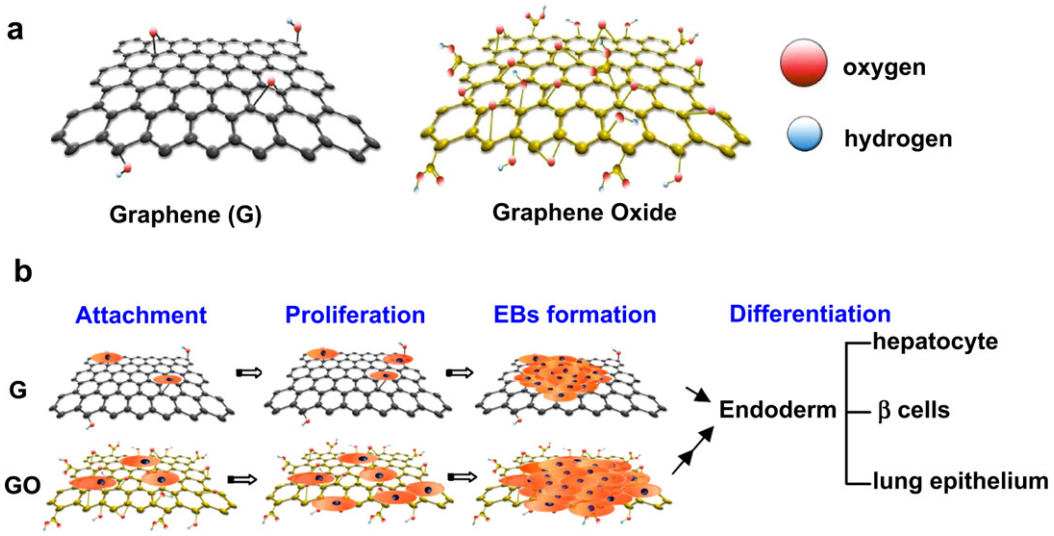

Fig. 9. Schematic illustration of (a) G and GO and (b) their use as a platform for iPSCs culture and differentiation.

nanosheets and differentially regulate the signal transduction pathways, thereby leading to the disparities in the differentiation propensity. To date the surface molecules and signal transduction pathways of iPSCs are poorly understood, thus the underlying mechanism contributing to this discrepancy remains to be investigated.

Altogether, we demonstrate the development of G and GO (Fig. 9a) as platforms for iPSCs culture and differentiation. Both G and GO surfaces supported the iPSCs culture, allowed for spontaneous differentiation, but led to different cell attachment, proliferation, EBs formation and differentiation characteristics, as summarized in Fig. 9b. This study underscored that the different surface properties of G and GO governed the iPSCs behavior. Moreover, our findings implicate the great potentials of G- and GO-coated materials as platforms for diverse biomedical applications. Given that G favors the maintenance of iPSCs pluripotency, G-coated substrates may be used for the subculture and expansion of iPSCs while obviating the need of feeder layer cells, which is crucial for future translation of the iPSCs technology to the clinics. Conversely, one can fabricate 3D porous, GO-coated scaffolds which, when coupled with the iPSCs induction medium, may preferentially and synergistically guide the iPSCs differentiation into cells along the endodermal lineage such as hepatocytes and insulin-producing β cells (Fig. 9b). Therefore, these GO-coated materials hold promise for the cell replacement therapy in acute liver failure/hepatitis and type I diabetes. In light of the effective transduction of iPSCs on the G- and GO-coated substrates, these nanomaterials also enable efficient genetic manipulation of iPSCs by viral vectors encoding appropriate factors to stimulate cellular differentiation.

5. Conclusions

In summary, hereby we developed G- and GO-coated biomaterials, which allow for attachment, proliferation and differential differentiation of iPSCs and hold great promise for iPSCs culture.

Acknowledgements

The authors acknowledge the generous gift of mouse iPSCs from Dr. Shinya Yamanaka (Center for iPS Cell Research and Application, Kyoto University) and the financial support from the National Tsing Hua University (Booster Program 99N2544E1 and Toward World-Class University Project 100N2050E1) and National Science Council (99-2221-E-007-025-MY3, 99-2221-E-007-096), Taiwan.

Appendix. Supplementary material

Supplementary data related to this article can be found online at doi:10.1016/j.biomaterials.2011.09.071.

References

[1] Rao CNR, Sood AK, Subrahmanyam KS, Govindaraj A. Graphene: the new two-dimensional nanomaterial. Angew Chem Int Ed 2009;48:7752–77.
[2] Novoselov KS, Geim AK, Morozov SV, Jiang D, Zhang Y, Dubonos SV, et al. Electric field effect in atomically thin carbon films. Science 2004;306:666–9.
[3] Cai Y, Li H, Du B, Yang M, Li Y, Wu D, et al. Ultrasensitive electrochemical immunoassay for BRCA1 using BMIM·BF4-coated SBA-15 as labels and functionalized graphene as enhancer. Biomaterials 2011;32:2117–23.
[4] Feng L, Chen Y, Ren J, Qu X. A graphene functionalized electrochemical aptasensor for selective label-free detection of cancer cells. Biomaterials 2011;32:2930–7.
[5] Markovic ZM, Harhaji-Trajkovic LM, Todorovic-Markovic BM, Kepic DP, Arsikin KM, Jovanovic SP, et al. In vitro comparison of the photothermal anticancer activity of graphene nanoparticles and carbon nanotubes. Biomaterials 2011;32:1121–9.
[6] Heo C, Yoo J, Lee S, Jo A, Jung S, Yoo H, et al. The control of neural cell-to-cell interactions through non-contact electrical field stimulation using graphene electrodes. Biomaterials 2011;32:19–27.
[7] Wang K, Ruan J, Song H, Zhang J, Wo Y, Guo S, et al. Biocompatibility of graphene oxide. Nanoscale Res Lett 2011;6:4317–23.
[8] Ryoo SR, Kim YK, Kim MH, Min DH. Behaviors of NIH-3T3 fibroblasts on graphene/carbon nanotubes: proliferation, focal adhesion, and gene transfection studies. ACS Nano 2010;4:6587–98.
[9] Chang Y, Yang ST, Liu JH, Dong E, Wang Y, Cao A, et al. In vitro toxicity evaluation of graphene oxide on A549 cells. Toxicol Lett 2010;200:201–10.
[10] Okita K, Ichisaka T, Yamanaka S. Generation of germline-competent induced pluripotent stem cells. Nature 2007;448:313–7.
[11] Yu JY, Vodyanik MA, Smuga-Otto K, Antosiewicz-Bourget J, Frane JL, Tian S, et al. Induced pluripotent stem cell lines derived from human somatic cells. Science 2007;318:1917–20.
[12] Wu SM, Hochedlinger K. Harnessing the potential of induced pluripotent stem cells for regenerative medicine. Nat Cell Biol 2011;13:497–505.
[13] Wernig M, Zhao JP, Pruszak J, Hedlund E, Fu D, Soldner F, et al. Neurons derived from reprogrammed fibroblasts functionally integrate into the fetal brain and improve symptoms of rats with Parkinson's disease. Proc Natl Acad Sci U S A 2008;105:5856–61.
[14] Xu D, Alipio Z, Fink LM, Adcock DM, Yang J, Ward DC, et al. Phenotypic correction of murine hemophilia A using an iPS cell-based therapy. Proc Natl Acad Sci U S A 2009;106:808–13.
[15] Hanna J, Wernig M, Markoulaki S, Sun CW, Meissner A, Cassady JP, et al. Treatment of sickle cell anemia mouse model with iPS cells generated from autologous skin. Science 2007;318:1920–3.

[16] Niwa H, Ogawa K, Shimosato D, Adachi K. A parallel circuit of LIF signalling pathways maintainspl uripotency of mouse ES cells. Nature 2009;460:118–22.
[17] Takahashi K, Tanabe K, Ohnuki M, Narita M, Ichisaka T, Tomoda K, et al. Induction of pluripotent stem cells from adult human fibroblasts by defined factors. Cell 2007;131:861–72.
[18] Kawabata K, Sakurai F, Yamaguchi T, Hayakawa T, Mizuguchi H. Efficient gene transfer into mouse embryonic stem cells with adenovirus vectors. Mol Ther 2005;12:547–54.
[19] Lo W-H, Hwang S-M, Chuang C-K, Chen C-Y, Hu Y-C. Development of a hybrid baculoviral vector for sustained transgene expression. Mol Ther 2009;17:658–66.
[20] Ho Y-C, Lee H-P, Hwang S-M, Lo W-H, Chen H-C, Chung C-K, et al. Baculovirus transduction of human mesenchymal stem cell-derived progenitor cells: variation of transgene expression with cellular differentiation states. Gene Ther 2006;13:1471–9.
[21] Zhou J, Zhang Y, Lin Q, Liu Z, Wang H, Duan C, et al. Embryoid bodies formation and differentiation from mouse embryonic stem cells in collagen/Matrigel scaffolds. J Genet Genomics 2010;37:451–60.
[22] Tomioka I, Maeda T, Shimada H, Kawai K, Okada Y, Igarashi H, et al. Generating induced pluripotent stem cells from common marmoset (Callithrix jacchus) fetal liver cells using defined factors, including Lin28. Genes Cells 2010;15:959–69.
[23] Ng ES, Azzola L, Sourris K, Robb L, Stanley EG, Elefanty AG. The primitive streak gene Mixl1 is required for efficient haematopoiesis and BMP4-induced ventral mesoderm patterning in differentiating ES cells. Development 2005;132:873–84.
[24] Sato T, Hidaka K, Iwanaga A, Ito M, Asano M, Nakabeppu Y, et al. Impairment of cardiomyogenesis in embryonic stem cells lacking scaffold protein JSAP1. Biochem Biophys Res Commun 2005;338:1152–7.
[25] Sadelain M. The need for genetically engineering therapeutic pluripotent stem cells. Mol Ther 2010;18:2039.
[26] Lin C-Y, Chang Y-H, Lin K-J, Yen T-Z, Tai C-L, Chen C-Y, et al. The healing of critical-sized femoral segmental bone defects in rabbits using baculovirus-engineered mesenchymal stem cells. Biomaterials 2010;31:3222–30.
[27] Lin C-Y, Lu C-H, Luo W-Y, Chang Y-H, Sung L-Y, Chiu H-Y, et al. Baculovirus as a gene delivery vector for cartilage and bone tissue engineering. Curr Gene Ther 2010;10:242–54.
[28] Hu W, Peng C, Lv M, Li X, Zhang Y, Chen N, et al. Protein corona-mediated mitigation of cytotoxicity of graphene oxide. ACS Nano 2011;5:3693–700.
[29] Wang K, Ruan J, Song H, Zhang J, Wo Y, Guo S, et al. Biocompatibility of graphene oxide. Nanoscale Res Lett 2011;6:4317–23.
[30] Nayak TR, Andersen H, Makam VS, Khaw C, Bae S, Xu X, et al. Graphene for controlled and accelerated osteogenic differentiation of human mesenchymal stem cells. ACS Nano 2011;5:4670–8.
[31] Liu Q, Shi J, Sun J, Wang T, Zeng L, Jiang G. Graphene and graphene oxide sheets supported on silica as versatile and high-performance adsorbents for solid-phase extraction. Angew Chem Int Ed 2011;50. doi:10.1002/anie.201007138.
[32] Mei Y, Saha K, Bogatyrev SR, Yang J, Hook AL, Kalcioglu ZI, et al. Combinatorial development of biomaterials for clonal growth of human pluripotent stem cells. Nat Mater 2010;9:768–78.
[33] Melkoumian Z, Weber JL, Weber DM, Fadeev AG, Zhou Y, Dolley-Sonneville P, et al. Synthetic peptide-acrylate surfaces for long-term self-renewal and cardiomyocyte differentiation of human embryonic stem cells. Nat Biotechnol 2010;28:606–10.
[34] Ma W, Tavakoli T, Derby E, Serebryakova Y, Rao MS, Mattson MP. Cell-extracellular matrix interactions regulate neural differentiation of human embryonic stem cells. BMC Dev Biol 2008;8:90.
[35] Wong JC, Gao SY, Lees JG, Best MB, Wang R, Tuch BE. Definitive endoderm derived from human embryonic stem cells highly express the integrin receptors alphaV and beta5. Cell Adh Migr 2010;4:39–45.
[36] Akasaka T, Yokoyama A, Matsuoka M, Hashimoto T, Watari F. Maintenance of hemiround colonies and undifferentiated state of mouse induced pluripotent stem cells on carbon nanotube-coated dishes. Carbon 2011;49:2287–99.
[37] Chao TI, Xiang S, Chen CS, Chin WC, Nelson AJ, Wang C, et al. Carbon nanotubes promote neuron differentiation from human embryonic stem cells. Biochem Biophys Res Commun 2009;384:426–30.